Main Group Element Size and Substitution Effects on the Structural Dimensionality of Zirconium Tellurides of the ZrSiS Type

Chwanchin Wang and Timothy Hughbanks*

Department of Chemistry, Texas A&M University, College Station, Texas 77843

Received April 26, 1995[⊗]

Chemical and structural variations in compounds related to the layered compound ZrSiTe have been examined. A study of $ZrSi_{1-x}Ge_xTe$ solid solutions show that the Si:Ge ratio can be varied in any stoichiometric proportion with the result that increasing atomic size (increasing x) affects both the shrinkage of the c axis and the expansion of the a axis. Expansion of the a axis results in relief of steric crowding within and between Te layers that permits increased bonding between Zr and Te in adjacent layers. This steric−electronic synergy is discussed. A new member of this structural family, ZnSnTe, was synthesized (space group $P4/nmm$, No. 129, $Z = 2$, a = 4.0549(6) Å, c = 8.711(2) Å). ZrSnTe has a fully three-dimensional structure; bond distances of Zr to the intralayer and interlayer Te, 3.038 and 3.084 Å, respectively, are almost equal. Four new pseudoternary tellurides are reported. Two of pseudoternary tellurides, $ZrSi_{0.66}As_{0.34}Te$ and $ZrSi_{0.5}As_{0.7}Te_{0.8}$, were refined in the same space group with lattice parameters a = 3.8116(1) Å, c = 8.398(3) Å for $ZrSi_{0.5}As_{0.7}Te_{0.8}$ and a = 3.7110(3) Å, c = 9.723(2) Å for $ZrSi_{0.66}As_{0.34}Te$. $ZrSi_{0.66}As_{0.34}Te$, isostructural with ZrSiTe, has a c axis length 0.22 Å larger than that of ZrSiTe; arsenic in this material substitutes solely for silicon. The isotypic $ZrSi_{0.5}As_{0.7}Te_{0.8}$ exhibits substitution for both Si and Te and can be formulated as $Zr(Si_{0.5}As_{0.5})(As_{0.2}Te_{0.8})$. Four-probe resistivity measurements (77−300 K) show all ternary and pseudoternary tellurides to be metallic with resistivities of $\sim 10^{-4}$ Ω cm.

Introduction

Over 200 MAB (M = transition metal; A, B = main group elements) compounds adopt a structure that is variously referred to as the Cu_2Sb, PbFCl, or ZrSiS structure type.[1−3] Described in general (purely geometric) terms, this tetragonal structure is built up by stacking five 4^4 square nets into slabs with a [B−M−$(A)_2$−M−B] stacking sequence. Because atoms of element A are packed into layers that are twice as dense as the B layers, it is common that there is appreciable A−A bonding and modest B−B bonding in compounds adopting this structure. Ternary compounds for which this description is appropriate fall into the "ZrSiS" category and are the subject of this paper.

Each zirconium in ZrSiS is surrounded by four silicon atoms and four sulfur atoms from the square nets bounding the Zr atom layer (Figure 1). In ZrSiS, zirconium is within bonding distance of a fifth sulfur atom that resides in the square net that is in the adjacent slab. In related compounds, the presence or absence of such interlayer bonding determines whether we describe the structure as "three-dimensional" or "layered", respectively. Silicon atoms sit in a square-planar environment of like silicon (at distance of 2.506 Å) and are bound to two Zr centers in the layers above and below, as indicated in Figure 1.

ZrSiS-type compounds offer interesting opportunities for tuning the structural dimensionality within a flexible structure type. In substitutions that leave the electron count constant, one may replace silicon with germanium (or tin—see below) or sulfur with selenium or tellurium. These substitutions provide the means to adjust a delicate steric−electronic balance that

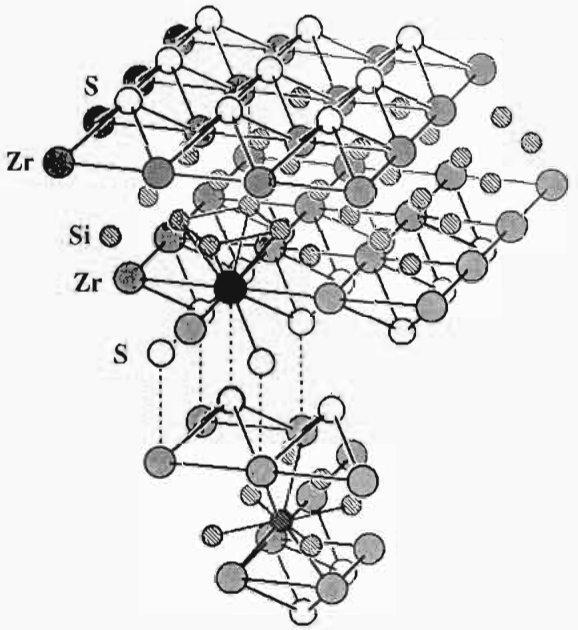

Figure 1. Structure of ZrSiS, built up with five 4^4 square nets into slabs with a [S−Zr−Si_2−Zr−S] stacking sequence. Shaded, open, and hatched atoms show the coordination environments of Zr, S, and Si in ZrSiS, respectively. The strength of interlayer bonds (dashed lines) determines whether the materials is "layered" or "three-dimensional".

governs the structural dimensionality of the compounds obtained. Thus, ZrSiS is a compound with a three-dimensional structure as described above, but ZrSiTe is a layered material without significant interlayer bonding. This mirrors the situation among PbFCl-type compounds; most LnOX (Ln = lanthanide; X = halide)[4] compounds exhibit structural changeover from a three-dimensional bonded structure to a true layered structure

* Author to whom correspondence should be addressed.

[⊗] Abstract published in *Advance ACS Abstracts*, October 1, 1995.

(1) Villars, P.; Calvert, L. D. *Pearson's Handbook of Crystallographic Data for Intermetallic Phases*, 3rd ed.; American Society for Metals: Materials Park, OH, 1985; Vol. 1, p 420.

(2) Haneveld, A. J. K.; Jellinek, F. *Recl. Trav. Chim. Pays-Bas* **1964**, *83*, 776.

(3) Onken, H.; Vierheilig, K.; Hahn, H. *Z. Anorg. Allg. Chem.* **1964**, *233*, 267.

(4) Hulliger, F. *Structural Chemistry of Layer-type Phases*; Reidel: Dordrecht, 1976; Vol. 5.

0020-1669/95/1334-5524$09.00/0

Table 1. *c/a* Ratios of Ternary Chalcogenides Isotypic with ZrSiS

compound	*c/a*	ref	compound	*c/a*	ref
ZrSiS	2.273	2, 3	SmSbTe	2.171	10
ZrSiSe	2.309	2, 3	GdSbTe	2.172	10
ZrSiTe	2.573	2, 3, 19	ThPS	2.213	5
ZrGeS	2.212	2, 3	ThPSe	2.029	5
ZrGeSe	2.232	2, 3	ThAsS	2.110	5
ZrGeTe	2.224	2, 3	ThAsSe	2.098	5
$Zr_2As_{1.9}S$	2.221	8, 9	ThAsTe	2.068	5
$Zr_2As_{2.3}Se$	2.165	8, 9	ThSbSe	2.083	5
$Zr_{1.4}As_2Te$	2.152	8	ThSbTe	2.094	5
$ZrSi_{0.66}As_{0.34}Te$	2.620	this work	ThBiTe	2.053	5
$ZrSi_{0.9}As_{0.4}Te_{0.7}$	2.282	this work	USiS	2.200	7
$ZrSi_{0.7}AsTe_{0.3}$	2.254	this work	UGeS	2.179	7
$ZrSi_{0.5}As_{0.7}Te_{0.8}$	2.203	this work	USnTe	2.144	7
ZrSnTe	2.148	this work	UPS	2.093	5
ZrSbTe	2.228	8	UPSe	2.072	5
HfSiS	2.273	3	UAsS	2.106	5
HfSiSe	2.292	3	UAsSe	2.103	5
HfSiTe	2.651	3	UAsTe	2.103	5
HfGeS	2.199	3	USbS	2.162	5
HfGeSe	2.222	3	USbSe	2.108	5
HfGeTe	2.196	3	USbTe	2.097	5
$Hf_{1.4}As_2S$	2.224	9	UBiTe	2.065	5
$Hf_{1.4}As_2Se$	2.193	9	NpAsS	2.153	6
$Hf_{1.4}As_2Te$	2.187	9	NpAsSe	2.158	6
LaSbTe	2.133	10	NpAsTe	2.152	6
CeSbTe	2.165	10	NpSbTe	2.121	10
PrSbTe	2.163	10	AmSbTe	2.124	10
NdSbTe	2.173	10	PuSbTe	2.124	10

as the size of halogen atoms increases on moving from Cl to Br to I. The *c/a* ratio, a useful indicator of this structural trend, is given for ternary chalcogenides isotypic with ZrSiS in Table 1. The tellurides MSiTe (M = Zr, Hf) have dramatically higher *c/a* ratios than corresponding sulfides or selenides MSiQ (M = Zr, Hf; Q = S, Se), and as truly layered compounds, they lie at the extreme in the range of *c/a* ratios. The 2-D to 3-D structural transformation occurs in a less direct, but no less dramatic, fashion when Si in ZrSiTe is replaced by Ge.[2]

Materials studied by Jeannin et al. with a nonstoichiometric composition in the ternary M−As−Q system (M = Zr, Hf; Q = S, Se, Te) exhibited a three-dimensionally bonded structure and could be formulated as $MAs_{1-x}(As_xQ_y)$.[8,9] These compounds showed exclusive As substitution in the chalcogenides' square nets and no marked differences of M−Q bond distances within (2.805 Å) and between layers (2.886 Å) in $Zr_2As_{2.30}Se_{1.15}$. This substitution phenomenon was not observed in the PbFCl-type compounds.

Interestingly, MAB compounds exhibit an electronically driven structural distortion of the A atom's square net in GdPS and CeAsS. Extended Hückel calculations showed that the ZrSiS-type structure had two bands crossing the Fermi level, yielding metallic behavior.[11] COOP curves[12−14] for P−P bonds exhibited large antibonding contributions below and above the Fermi level in GdPS with an assumed ZrSiS structure. In order to avoid P−P antibonding, the phosphorus square net undergoes a deformation to form cis−trans polyphosphide chains, which opens a band gap and results in a semiconducting material. A similar phenomenon is manifest in CeAsS, but its As square net distorts into zigzag polyarsenic chains.

There are some questions remaining unanswered concerning ZrSiS-type compounds. First, a 2-D to 3-D structural transformation is observed in ZrSiTe and ZrGeTe. We were interested in discovering whether segregation of different structure types occurs in the $ZrSi_{1-x}Ge_xTe$ solid solution. Second, the synthesis of ZrSnTe should allow us to verify the size effect on the 2-D to 3-D structural transformation. Third, there are questions about whether substitution of arsenic in the chalcogenide square net will occur for the telluride compounds. Si and As have comparable atomic sizes, and we wished to investigate whether $ZrSi_{1-x}As_xTe$ solid solutions behave like $ZrSi_{1-x}Ge_xTe$ solid solutions. Such a study is presented in this paper. We also report the synthesis of several new materials isostructural with either ZrSiTe or ZrGeTe.

Experimental Section

Synthesis. Since most of the product tellurides described herein are sensitive to both moisture and oxygen, the operations described below were performed under nitrogen atmosphere. Elemental starting materials, Zr (99.2%, including 4.5% Hf, Johnson Matthey), As (99.99%, Alfa), Si (99.999%, Aldrich), Ge (99.999%, Aldrich), Ga (99.999%, Johnson Matthey), Sn (99.9%, Baker), and Te (99.99%, Johnson Matthey), were used as received.

$ZrSi_{1-x}Ge_xTe$ solid solutions were prepared by directly mixing elements in stoichiometric proportions. Materials with eight different compositions were prepared (x = 0.0, 0.15, 0.33, 0.5, 0.67, 0.75, 0.85, 1.0) by mixing appropriate amounts in individual silica ampules. In each case, the reaction temperature was raised to 550 °C over 5 h and maintained at that temperature for 2 days. The temperature was then raised to 850 °C over a 24 h interval, maintained at 850 °C for another 4 days, and then quenched to room temperature. Microprobe analysis of the products gave compositions that were reasonably consistent with loaded compositions: $ZrSi_{0.97(2)}Te_{0.99(1)}$ (x = 0.0), $ZrSi_{0.77(1)}Ge_{0.18(1)}Te_{0.99(1)}$ (x = 0.15), $ZrSi_{0.70(4)}Ge_{0.31(2)}Te_{0.94(3)}$ (x = 0.33), $ZrSi_{0.49(1)}Ge_{0.49(1)}Te_{0.95(1)}$ (x = 0.50), $ZrSi_{0.33(1)}Ge_{0.63(1)}Te_{0.94(1)}$ (x = 0.67), $ZrSi_{0.24(1)}Ge_{0.74(2)}Te_{0.98(2)}$ (x = 0.75), $ZrSi_{0.13(1)}Ge_{0.85(2)}Te_{1.00(3)}$ (x = 0.85), $ZrGe_{1.02(1)}Te_{1.01(1)}$ (x = 1.0). Procedures and conditions used in preparing $ZrSi_{1-x}As_xTe$ solid solutions were the same as those for $ZrSi_{1-x}Ge_xTe$. Materials with five different compositions were prepared (x = 0.0, 0.33, 0.5, 0.67, 1.0).

The synthesis of ZrSnTe was initially attempted by mixing elements in a 1:1:1 ratio with the transport reagent $TeCl_4$ in a quartz tube. The temperature was raised to 550 °C over 6 h and maintained at 550 °C for 4 days. It was then raised to 900 °C over 12 h and then maintained for 21 days in a 900−950 °C temperature gradient. The product consisted entirely of black square plate crystals that were identified as ZrSiTe by inspection of Guinier powder diffraction patterns. However, ZnSnTe was serendipitously synthesized when a Sn flux was used in a reaction mixture that had been loaded with elemental starting materials at the "Zr_3Te_2B" composition. Sn and the "Zr_3Te_2B" mixture were combined in a 1:1 ratio and loaded into a niobium tube which was in turn sealed in an evacuated ($\sim 10^{-4}$ Torr) silica ampule. The reaction temperature was uniformly raised to 550 °C over 36 h and maintained at 550 °C for 2 days. The temperature was then uniformly raised to 950 °C over a 3 day interval and maintained at 950 °C for 21 days. The reaction mixture was then cooled from 950 to 400 °C at a rate of 4 °C/h, and the furnace was subsequently turned off to cool to room temperature. Many large square-faceted crystals were found in the product. Microprobe analysis of these crystals gave the composition $ZnSn_{1.07(7)}Te_{0.98(6)}$—no boron was detected. ZrSnTe was subsequently synthesized (in a Nb tube, as above) in the absence of boron with the elements mixed in a 1:1:1 ratio. The product was always found to be contaminated with a minor amount of $ZrTe_2$.

In a reaction designed to form an isoelectronic "GaAs" layered compound ($ZrGa_{0.5}As_{0.5}Te$), isoelectronic with ZrSiTe, elemental Zr, Ga, As, and Te were combined in a molar ratio of 2:1:1:2 (total mass 0.3 g) along with 3 mg of $TeCl_4$ and sealed in a 10 cm long quartz

(5) Hulliger, F. *J. Less-Common Met.* **1986**, *16*, 113−117.
(6) Wojakowski, A. *J. Less-Common Met.* **1985**, *107*, 155−158.
(7) Haneveld, A. J. K.; Jellinek, F. *J. Less-Common Met.* **1969**, *18*, 123−129.
(8) Barthelat, J.-C.; Jeannin, Y.; Rancurel, J.-F. *C. R. Acad. Sci. Paris* **1969**, *268*, 1756.
(9) Barthelat, J. C.; Jeannin, Y. *J. Less-Common Met.* **1972**, *26*, 273.
(10) Wojakowski, A. *Rev. Chim. Miner.* **1977**, *14*, 178.
(11) Tremel, W.; Hoffmann, R. *J. Am. Chem. Soc.* **1987**, *109*, 124.
(12) Hughbanks, T.; Hoffmann, R. *J. Am. Chem. Soc.* **1983**, *105*, 3528.
(13) Wijeyesekera, S. D.; Hoffmann, R. *Organometallics* **1984**, *3*, 949.
(14) Hoffmann, R. *Solids and Surfaces: A Chemist's View of Bonding in Extended Structures*; VCH Publishers, Inc.: New York, 1988.

Table 2. Crystallographic Data for $ZrSi_{0.66}As_{0.34}Te$, $ZrSi_{0.5}As_{0.7}Te_{0.8}$, and ZrSnTe

	$ZrSi_{0.66}As_{0.34}Te$	$ZrSi_{0.5}As_{0.7}Te_{0.8}$	ZrSnTe
a, Å	3.7110(3)	3.8116(1)	4.0549(6)
c, Å	9.723(2)	8.398(3)	8.711(2)
V, Å^3	133.90(3)	122.03(6)	143.24(6)
Z	2	2	2
fw	262.83	259.79	336.99
space group	*P4/nmm* (No. 129)	*P4/nmm* (No. 129)	*P4/nmm* (No. 129)
T (°C)	20	20	20
λ (Å)	0.710 73	0.710 73	0.710 73
ϱ_{calcd}, g/cm^3	6.484	7.151	7.826
μ (mm^{-1})	18.509	23.457	21.978
no. of unique reflns	97 (R_{int} = 8.11%)	197 (R_{int} = 3.74%)	229 (R_{int} = 7.80%)
no. of unique obsd reflns, $F_o^2 > 2\sigma(F_o^2)$	96	186	224
no. of variables	12	14	10
R^a	0.014	0.036	0.025
$R_w{}^b$	0.027	0.092	0.050
GOF	1.473	1.536	1.369

^{a} $R(F) = \sum(||F_o| - |F_c||)/\sum(|F_o|)$. ^{b} $R_w(F^2) = \{\sum[w(F_o^2 - F_c^2)^2]/\sum[w(F_o^2)^2]\}^{1/2}$; $w = 1/[\sigma^2(F_o^2) + (xP)^2 + yP]$ where $P = (\mathrm{Max}(F_o^2,0) + 2F_c^2)/3$. In each case: $x = 0.0$, $y = 0.1739$ for $ZrSi_{0.66}As_{0.34}Te$; $x = 0.0369$, $y = 4.0776$ for $ZrSi_{0.5}As_{0.7}Te_{0.8}$; $x = 0.0063$, $y = 0.7105$ for ZrSnTe.

tube coated with pyrolytic carbon. The temperature was raised to 550 °C over 5 hours, maintained at 550 °C for 3 days, raised to 900 °C over 3 days, and then subjected to a 900−950 °C temperature gradient for 35 days. The reaction mixture was cooled by turning off the furnace and allowing it to cool to room temperature. After this prolonged reaction, the silica ampule was devitrified and several plate crystals up to millimeter size were obtained. The microprobe analysis (Cameca SX-50) on selective crystals showed the approximate composition $ZrSi_{0.66(1)}As_{0.34(2)}Te_{0.97(1)}$. Unreacted gallium droplets were observed in the product; no other elements heavier than Na were found. The quantitative synthesis of $ZrSi_{0.66}As_{0.34}Te$ can be achieved by mixing elements in a stoichiometric proportions and conducting the reaction in the manner described in the preparation of solid solutions of $ZrSi_{1-x}Ge_xTe$.

Zr−Si−As−Te materials structurally isotypic with ZrGeTe were prepared in silica ampules by mixing 0.3 g of a Zr, As, Si, and Te mixture in a ratio of 4:3:1:4 with 3 mg of $TeCl_4$. The reaction temperature was brought up to 550 °C in 5 h and kept there for 2 days. It was then raised to 1000 °C over 12 h, and a temperature gradient was applied in the range of 1000−950 °C for 3 weeks. Several plate crystals were found in the product. Selected plate crystals were analyzed by microprobe analysis, which gave the approximate composition $ZrSi_{0.48(1)}As_{0.70(1)}Te_{0.79(3)}$. Subsequently, the composition found by microprobe analysis was used to obtain a single-phase product with the composition $ZrSi_{0.5}As_{0.7}Te_{0.8}$. Conditions for this synthesis were as described above in the preparation of $ZrSi_{1-x}Ge_xTe$ solid solutions. In an attempt to grow single crytals of this phase by use of a Sn flux, 0.6 g of a mixture of elemental Zr, Si, As, Te, and Sn in a ratio of 1:0.5:0.7:0.8:1 was mixed with 3 mg of $TeCl_4$. The reaction temperature was raised to 550 °C over a 6 h interval and maintained there for 3 days. It was then raised to 900 °C over 12 h, and a 900−950 °C temperature gradient was applied for another 21 days before allowing the furnace to cool to room temperature. Microprobe analysis of selected plate crystals gave the approximate composition $ZrSi_{0.8(1)}As_{0.47(2)}Te_{0.74(2)}$. No other elements heavier than Na were found in any of the products described above. A quantitative synthesis (by analysis) of $ZrSi_{0.9}As_{0.5}Te_{0.7}$ could be achieved by mixing elements in stoichiometric proportions.

In an attempt to synthesize $ZrSi_{0.5}AsTe_{0.5}$, a reaction run by mixing elements in a ratio of 1:0.5:1:0.5 with 3 mg of $TeCl_4$ was conducted in a silica ampule. The reaction temperature was raised to 550 °C over 1 h and kept there for 2 days. It was then raised to 900 °C over 12 h, and a 900−950 °C temperature gradient was applied for another 21 days before allowing the furnace to cool to warm temperature. Microprobe analysis of selected plate crystals gave the approximate composition $ZrSi_{0.74(2)}As_{0.97(3)}Te_{0.37(2)}$.

X-ray Studies. Two black plate crystals of $ZrSi_{0.66}As_{0.34}Te$ and $ZrSi_{0.5}As_{0.7}Te_{0.8}$ and a black chunk crystal of ZnSnTe of approximate dimensions 0.31 × 0.20 × 0.07 mm, 0.30 × 0.28 × 0.04 mm and 0.30 × 0.20 × 0.16 mm, respectively, were selected and mounted in glass capillaries. Preliminary oscillation and Weissenberg photographs were used to establish tetragonal unit cells and to obtain approximate lattice parameters. Cell parameters refined from Guinier powder diffraction patterns for all three compounds are given in Table 2. Single-crystal X-ray data were collected for each on a Siemens R3m/V diffractometer with graphite-monochromated Mo Kα radiation at 20 °C. Tetragonal cell constants and an orientation matrix were obtained in each case from a least-squares refinement using 24 centered reflections in the range of $20 \le 2\theta \le 35°$. Intensity data were collected in the $\theta-2\theta$ scanning mode for reflections with $4 < 2\theta < 50°$ for $ZrSi_{0.66}As_{0.34}Te$ and $4 < 2\theta < 70°$ for both $ZrSi_{0.5}As_{0.7}Te_{0.8}$ and ZrSnTe. One quadrant of data was collected $(+h,+k,\pm l)$ for $ZrSi_{0.66}As_{0.34}Te$. A hemisphere $(+h,\pm k,\pm l)$ of data was collected for both $ZrSi_{0.5}As_{0.7}Te_{0.8}$ and ZrSnTe to gain the advantage of averaging. In each case, three check reflections were monitored periodically and showed no significant change during the data collection process. $ZrSi_{0.5}As_{0.7}Te_{0.8}$ and ZrSnTe data sets were corrected for absorption using the ψ-scan technique on the basis of three and five reflections, respectively. An absorption correction using six measured faces was applied to the $ZrSi_{0.66}As_{0.34}Te$ data. The systematic absences $h + k = 2n + 1$ for $(hk0)$ are consistent with the space group *P4/n* (No. 86) and *P4/nmm* (No. 129). Since these tellurides are isostructural with either ZrSiTe or ZrGeTe according to Guinier powder diffraction patterns, the atomic positions of ZrSiTe were used to refine the atomic positions of $ZrSi_{0.66}As_{0.34}Te$ and those of ZrGeTe were used to refine the atomic positions of both ZrSnTe and $ZrSi_{0.5}As_{0.7}Te_{0.8}$. Refinements of both space groups showed the same results; thus the centrosymmetric space group *P4/nmm* was chosen for the crystallographic analysis.

The structure refinements were based on F^2 with the use of the SHELX-93 program.[15] For all three structures, neutral atomic scattering factors, corrected for the real and imaginary parts of anomalous dispersion, were obtained from standard sources.[16] Isotropic refinement of ZrSnTe showed reasonable thermal coefficients for all atoms. Anisotropic refinement of ZrSnTe gave the final residual $R = 2.52\%$ with the largest remaining peak 0.7 Å near the Sn position. When $ZrSi_{0.66}As_{0.34}Te$ was refined isotropically under the assumption that only Zr, As, and Te atoms were present, the As thermal coefficient was about 5 times larger than that of Zr and a residual $R = 8.52\%$ was obtained. Partial Si occupancy of the As site was introduced subject to the constraints that the summed Si and As occupancies were unity (i.e., the composition was $Zr(Si_xAs_{1-x})Te$) and that these atoms' thermal parameters were equal. This yielded a residual (R) of 4.91%, a silicon occupancy of 69%, and thermal coefficients for the As (Si) atoms that were 1.5 times larger than that of Zr. After correction for absorption with DIFABS,[17] anisotropic refinement of $ZrSi_{0.66}As_{0.34}Te$ showed the thermal ellipsoids of all atoms to be fairly isotropic and gave the final

(15) Sheldrick, G. M. *SHELX-93*; Nicolet Analytical X-ray Instruments: Göttingen, Germany, 1993.
(16) *International Tables for X-ray Crystallography*; Ibers, J. A.; Hamilton, W. C., Eds.; Kynoch Press: Birmingham, England, 1974; Vol. IV.
(17) Walker, N.; Stuart, D. *Acta Crystallogr.* **1983**, *A39*, 158.

Table 3. Atomic Coordinates and Equivalent Isotropic Displacement Parameters

atom	x	y	z	U_{eq}[a] (Å × 10^3)
		$ZrSi_{0.66}As_{0.34}Te$		
Zr	0.25	0.25	0.2157(1)	9(1)
Te	0.25	0.25	0.6470(1)	10(1)
Si/As	0.75	0.25	0.0	12(1)
		$ZrSi_{0.5}As_{0.7}Te_{0.8}$		
Zr	0.25	0.25	0.2469(2)	12(1)
Te/As1	0.25	0.25	0.6223(1)	10(1)
Si/As2	0.75	0.25	0.0	16(1)
		ZrSnTe		
Zr	0.25	0.25	0.2652(1)	4(1)
Te	0.25	0.25	0.6195(1)	4(1)
Sn	0.75	0.25	0.0	6(1)

[a] Equivalent isotropic U defined as one-third of the trace of the orthogonalized $\mathbf{U}_{ij}$ tensor.

residual $R = 1.43\%$. The largest remaining peak in the final difference Fourier map was about 1.7 Å from the Te atom. Isotropic refinement of $ZrSi_{0.5}As_{0.7}Te_{0.8}$ assuming a ZrAsTe composition resulted in a residual $R = 6.91\%$; the thermal coefficient for Te was a bit smaller than that for Zr, and the thermal parameter for the As atom was about 2 times larger than that for Zr. Both the As and Te site occupanices were allowed to vary as follows: the As site was refined with both As and Si; the Te site was refined with both As and Te (i.e., a $Zr(Si_x As_{1-x})(As_y Te_{1-y})$ model was used). This yielded a silicon occupancy of 47%, arsenic occupanices of 53% in the Si site and 17% in the Te site, and a tellurium occupancy of 83%. These results were well matched with those from the microprobe analysis. The refinement led to a final residual $R = 4.41\%$ and reasonable thermal parameters for all atoms. Anisotropic refinement of $ZrSi_{0.5}As_{0.7}Te_{0.8}$ gave the final residual $R = 3.63\%$, with the largest remaining peak 0.65 Å from the Te atom. A summary of crystal and data collection parameters is given in Table 2, and final atomic coordinates are located in Table 3.

Electrical Resistivity Measurements. All ternary and pseudoternary tellurides are sensitive to air and moisture; resistivity measurements were thus carried out under an atmosphere of dry nitrogen. Resistivities were measured using a dc four-probe method; contacts were made with silver epoxy (Acme E-solder 3021), and leads from the contacts consisted of 0.05 mm diameter gold wires. Except for ZrSnTe, resistivities were only measured parallel to the *ab* plane. Crystals generally exhibit a square-plate morphology, and screw dislocations parallel to the 4-fold axis could be viewed in the microscope. All measurements were repeated at least twice on separate crystals. Temperature equilibration was ensured by carrying out measurements with both cooling and warming over the range 77−300 K. Crystal dimensions necessary to obtain the absolute resistivities were measured with a Zeiss Laser scanning microscope (LSM-10). The absolute resistivities of ternary and pseudoternary tellurides at 273 K, 3.1×10^{-4} Ω cm (ZrSiTe), 7.2×10^{-5} Ω cm (ZrSnTe), 1.1×10^{-4} Ω cm ($ZrSi_{0.66}As_{0.34}Te$), 1.5×10^{-4} Ω cm ($ZrSi_{0.5}As_{0.7}Te_{0.8}$), and 1.0×10^{-4} Ω cm ($ZrSi_{0.7}AsTe_{0.3}$), were calculated with measured crystals dimensions 24 μm × 0.2 mm × 0.28 mm, 27 μm × 0.18 mm × 71 μm, 38 μm × 0.45 mm × 0.19 mm, 19 μm × 0.39 mm × 0.23 mm, and 46 μm × 0.48 mm × 0.22 mm, respectively.

Results and Discussion

Syntheses. The synthesis of reduced binary or ternary zirconium chalcogenides in silica tubes often leads to the formation of zirconium silicide chalcogenides, ZrSiQ (Q = S, Se, Te) and zirconium silicate, $ZrSiO_4$, in prolonged reactions. Despite the convenience and usefulness of silica as containers in solid-state synthesis, the incorporation of the Si or SiO_2 from a quartz tube at high temperature (>800 °C) has often served, unintentionally or intentionally, as a source of Si in new materials. The pseudoternary telluride $ZrSi_{0.66}As_{0.34}Te$, for example, was serendipitously obtained with the attack of the silica ampule at 950 °C when a reaction mixture was loaded with only elemental Zr, Ga, As, and Te. $ZrSi_{0.66}As_{0.34}Te$ could later be quantitatively synthesized by mixing elements in a stoichiometric proportion.

Jellinek et al. found that ZrSnTe could not be successfully synthesized in a silica ampule.[7] Similarly, we find that the attempted synthesis of ZrSnTe in a silica ampule yields only ZrSiTe. To avoid the incorporation of Si from a silica ampule, niobium metal tubes were employed. In an attempt to grow crystals of a boron-containing compound by use of the Sn flux in a niobium tube, ZrSnTe was serendipitously obtained. Direct mixing of elements in stoichiometric proportions yields ZrSnTe in about 80% yield, with $ZrTe_2$ forming the rest of the product. Guinier powder patterns of ZrSnTe obtained in this manner and of the original boron-containing reaction mixture are superimposable, excluding the possibility of boron in the ZrSnTe obtained in the original synthesis. Several attempts to synthesize ZrSnQ (Q = S, Se) and HfSnTe in niobium tubes by directly mixing elements were unsuccessful.

Because ZrSiTe was obtained in an attempt to synthesize ZrSnTe in a silica ampule, the Sn flux was purposely added to aid in growing single crystals of $ZrSi_{0.5}As_{0.7}Te_{0.8}$. Interestingly, the reaction resulted in formation of another pseudoternary telluride, $ZrSi_{0.9}As_{0.4}Te_{0.7}$, which is also isotypic with ZrGeTe by comparison of Guinier powder diffraction patterns. In an attempt to increase the As content in the pseudoternary compounds, a reaction with a higher As content (composition $ZrSi_{0.5}As_{1.0}Te_{0.5}$) was conducted and yielded another As-rich pseudoternary telluride, $ZrSi_{0.7}AsTe_{0.3}$. This compound was found to be isostructural with ZrGeTe.

$ZrSi_{1-x}Ge_xTe$ Solid Solutions. ZrSiTe and ZrGeTe are isostructural with ZrSiS (Figure 1); however, ZrGeTe has a three-dimensional structure while a layered structure holds for ZrSiTe. The main structural difference involves the Zr coordination environment: the interlayer Zr−Te distance in ZrSiTe is too long (3.948 Å) for any significant bonding while a substantial bond (3.26 Å) exists in ZrGeTe (Table 4). The larger atomic size of Ge dictates that the longer Ge−Ge bonds are appropriate for the germanium square net in ZrGeTe. This necessitates a corresponding increase in the in-plane Te−Te spacing at the exterior of the $Te-Zr-Ge_2-Zr-Te$ slab. This increased spacing apparently allows Te atoms in the adjacent slabs to approach more closely for the formation in interlayer Zr−Te bonds.

We conducted solid solution studies to determine whether the Te−Te spacing would show a smooth variation with Ge content or whether phase segregation driven by structural mismatch would occur. $ZrSi_{1-x}Ge_xTe$ solid solutions with eight different compositions were prepared in silica ampules. We were a bit surprised to learn that no segregation into two phases occurs. The analytical results showed that Si and Ge could be mixed in any stoichiometric proportion. The sharp Guinier powder diffraction lines are indicative of a homogeneous Si/Ge mixing in the compounds. The plot of lattice parameters vs Ge content (atom percent) is shown in the Figure 2. Numerical data for Figure 2 are available as Supporting Information. As the Ge content increases from 0% to 100%, the *c* axis length smoothly decreases from 9.469 Å (ZrSiTe) to 8.593 Å (ZrGeTe) and the *a* axis length increases from 3.6903 Å (ZrSiTe) to 3.8661 Å (ZrGeTe). These results indicate that gradually increasing the Ge content simultaneously lengthens the Si(Ge)−Si(Ge) bond distances in the *ab* plane with an accompanying diminution of the Te−Te steric crowding (the Te−Te distance is equal to $2^{1/2}d$(Si(Ge)−Si(Ge))). This allows the Te in adjacent layers to move toward the Zr with the formation of the interlayer Zr−Te bonds (Figure 3). The cell

Table 4. Cell Parameters and Interatomic Distances of Pseudoternary and Ternary Tellurides (Å)

compound	*a*	*c*	Zr−4Te$_i$[a]	Zr−Te$_o$	Te$_i$−Te$_o$	Zr−4X[b]	X−X	ref
$ZrSi_{0.66}As_{0.34}Te$	3.7110(3)	9.723(2)	2.944(1)	4.194(1)	3.881(1)	2.801(1)	2.624(1)	this work
ZrSiTe	3.6974(9)	9.508(2)	2.918(1)	3.957(1)	3.730(1)	2.819(1)	2.614(1)	19
ZrSiTe[c]	3.6903(1)	9.496(2)	2.912(1)	3.948(1)	3.722(1)	2.816(1)	2.609(1)	this work
ZrGeTe	3.866(2)	8.599(4)	2.93(1)	3.26(4)	3.51(3)	2.88(2)	2.734(1)	2
$ZrSi_{0.9}As_{0.4}Te_{0.7}$	3.7464(7)	8.549(4)						this work
$ZrSi_{0.5}As_{0.7}Te_{0.8}$	3.8116(1)	8.398(3)	2.911(1)	3.153(1)	3.389(1)	2.816(1)	2.696(1)	this work
$ZrSi_{0.7}AsTe_{0.3}$	3.7020(4)	8.346(2)						this work
ZrSnTe	4.0549(6)	8.711(2)	3.038(1)	3.086(1)	3.544(1)	3.074(1)	2.867(1)	this work
USnTe	4.2596(3)	9.1313(4)	3.142(3)	3.24(1)	3.82(1)	3.252(3)	3.012(1)	7

[a] i denotes the intralayer, and o denotes the interlayer. [b] X denotes the post-transition metals (Si, Ge, As, Sn). [c] The cell constants were obtained from Guinier powder diffraction using Si as an internal standard.

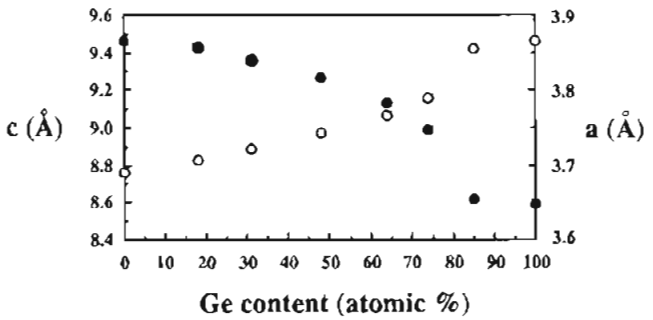

Figure 2. Changes in *c* (filled circles) and *a* (open circles) axes with increasing Ge content in $ZrSi_{1-x}Ge_xTe$ solid solutions. Errors are ≤0.0007 Å for *a* and 0.003 Å for *c*, too small to indicate in the figure.

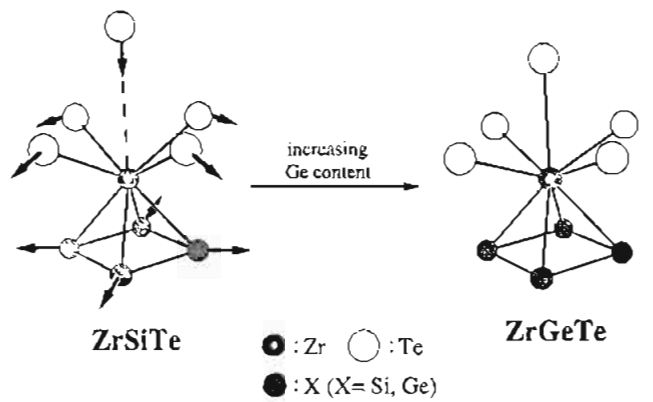

Figure 3. Interplay between bonding within and between layers in the $ZrSi_{1-x}Ge_xTe$ system. Increasing Ge content gradually decreases the steric crowding between Te atoms, allowing a closer approach between layers.

volume of each compound remains roughly constant (to within 1.5%) while the *c*/*a* ratio decreases from 2.566 (ZrSiTe) to 2.211 (ZrGeTe).

Crystal Structure of ZrSnTe. ZrSnTe was successfully obtained by the use of a niobium metal tube as a container. The cell parameters and important bond distances are listed in Table 4. ZnSnTe is isostructural with ZrGeTe, but the coordination environment of Zr is much more regular with respect to Zr−Te distances. There is an estimated 0.33 Å difference in the interlayer and intralayer Zr−Te bond distances in the ZrGeTe; this difference shrinks to only 0.05 Å in ZrSnTe (3.086 and 3.038 Å). ZnSnTe is thus fully three-dimensional. The Sn is coordinated to four zirconium atoms in a distorted tetrahedron, each at a distance of 3.074 Å, and to four Sn atoms in the square net at a distance of 2.867 Å (comparable to that of α-Sn, 2.810 Å). It is interesting that ZrSnTe exhibits significantly shorted "interlayer" Te−Te distances than the two-dimensional compounds, ZrSiTe and $ZrSi_{0.66}As_{0.34}Te$ (Table 4). The Guinier powder film of ZrSnTe shows five weak lines that can be indexed with a doubling of the *a* and *c* axes, yet no superlattice peaks could be observed in our single-crystal study. ZnSnTe is also isostructural with USnTe,[7] for which cell constants and interatomic distances are listed in the Table 4.

In summary, the compound ZrSnTe completes the 2-D to 3-D transformation that is well underway on moving from ZrSiTe to ZrGeTe—this is clearly due to the increase in atomic size on moving down the group 14 elements. The *c*/*a* ratios shown for this family decrease from 2.573 (Si) to 2.224 (Ge) to 2.148 (Sn), which parallels the trend in the ZrSiQ (Q = S, Se, Te) family (Table 1).

$ZrSi_{1-x}As_xTe$ Solid Solutions. An attempt to modify the "Si_2" square nets in ZrSiTe by substituting with "GaAs" led to the formation of a pseudoternary compound $Zr(Si_{0.66}As_{0.34})Te$, with a mixed "$(Si_{0.66}As_{0.34})_2$" square net. This outcome prompted us to investigate the $Zr(Si_{1-x}As_x)Te$ solid solutions. Five different compositions (x = 0.0, 0.33, 0.50, 0.67, 1.0) of $ZrSi_{1-x}As_xTe$ solid solutions were prepared. Unlike the results obtained from the Zr−Si−Ge−Te solid solution studies, disproportionation was observed in these studies; some crystalline compounds were isolated and structurally characterized. When x was equal to 0.33, the only observed product was isostructural with ZrSiTe and its structure was determined to be a two-dimensional compound, $ZrSi_{0.66}As_{0.34}Te$ (see below). As x was increased to 0.5, disporportionation occurred, the products being $ZrSi_{0.66}As_{0.34}Te$ and a member of the $Zr(Si_{1-x}As_x)(As_yTe_{1-y})$ ($0 \le x, y < 1$) solid solution (whose exact composition is not known). When x was 0.67, disporportionation again occurred to yield $Zr_4As_3Te_5$[18] and another member that was a representative of the $Zr(Si_{1-x}As_x)(As_yTe_{1-y})$ ($0 \le x, y < 1$) solid solution with the composition $ZrSi_{0.5}As_{0.7}Te_{0.8}$. The only observed As-containing product of the last reaction (x = 1.0) was $Zr_4As_3Te_5$.

Crystal Structures of $ZrSi_{0.66}As_{0.34}Te$ and $ZrSi_{0.5}As_{0.7}Te_{0.8}$. The cell parameters and important bond distances of the two title compounds are listed in Table 4. The pseudoternary zirconium telluride, $ZrSi_{0.66}As_{0.34}Te$, is isostructural with ZrSiTe and consists of five 4^4 square nets in each layer with a [Te−Zr−$(Si_{0.66}As_{0.34})_2$−Zr−Te] stacking sequence. Arsenic in this compound substitutes only for silicon; X-ray diffraction data are inconsistent with appreciable substitution for tellurium. The Zr−Te and Zr−Si(As) bond distances, 2.944 and 2.801 Å, are respectively 0.032 Å longer and 0.015 Å short than that for the ternary silicon parent compound. The interlayer Zr−Te bond distance, 4.194 Å, is even longer (0.25 Å) than that of ZrSiTe, so that $ZrSi_{0.66}As_{0.34}Te$ is a true layered compound. The closest Te−Te contact distance within the layers is 3.711 Å. The closest interlayer Te−Te contact is even longer at 3.881 Å. The Si(As)−Si(As) distance is 2.624 Å, 0.015 Å longer than the Si−Si distance in ZrSiTe.

$ZrSi_{0.5}As_{0.7}Te_{0.8}$ is isostructural with ZrGeTe and can be

(18) Mosset, A.; Jeannin, Y. *J. Less-Common Met.* **1972**, *26*, 285.
(19) Bensch, W.; Dürichen, P. *Acta Crystallogr.* **1994**, *C50*, 346−348.

formulated as $Zr(Si_{0.5}As_{0.5})(As_{0.2}Te_{0.8})$, consistent with X-ray diffraction and microprobe analytical results. In this material, As substitutes at both Si and Te sites. Both Zr−Te(As) and Zr−Si(As) bond distances, 2.911 and 2.816 Å, are coincidentally equal to corresponding distances in ZrSiTe. However, the interlayer Zr−Te(As) bond distance of 3.153 Å is shorter by 0.8 Å than the corresponding Zr−Te distance in ZrSiTe. This drastic shrinkage indicates the formation of interlayer bonds, despite the fact that only 20% of Te is replaced by As. The Si(As)−Si(As) bond distance is lengthened by 0.09 Å compared with that of ZrSiTe. It would appear that the layer expansion in the *ab* plane is driven by the formation of interlayer bonds since only a small expansion occurs in $ZrSi_{0.66}As_{0.34}Te$. There is a corresponding decrease in the interlayer Te(As)−Te(As) contact distance, 3.389 Å.

Two members belonging to the $Zr(Si_{1-x}As_x)(As_yTe_{1-y})$ ($0 \leq x, y < 1$) solid solution with different compositions (by microprobe analysis) were also obtained by different synthetic routes: $ZrSi_{0.9}As_{0.4}Te_{0.7}$ and $ZrSi_{0.7}AsTe_{0.3}$. These can be formulated as $Zr(Si_{0.9}As_{0.1})(As_{0.3}Te_{0.7})$ and $Zr(Si_{0.7}As_{0.3})(As_{0.7}Te_{0.3})$. Their cell parameters are listed in the Table 4. The complexity introduced by As substitution on both the Si and Te sites makes it difficult to rationalize all the structural changes observed. Nevertheless, it is clear that, owing to the As substitution in Te layers, all these compounds exhibit three-dimensionally bonded structures with formation of interlayer bonds. The replacement of chalcogenides with As in layered compounds also occurs in the ternary zirconium arsenide chalcogenides $Zr_2As_{2.30}S$,[9] $Zr_2As_{2.30}Se_{1.15}$,[9] and $Zr_{1.4}As_2Te$.[8]

The expansion of the Si layers upon As doping is not entirely explained by the shrinkage of the *c* axis length in the $Zr(Si_{1-x}As_x)(As_yTe_{1-y})$ ($0 \leq x, y < 1$) materials. Partial substitution with As into the Si layers causes a modest increase in the *a* axis length (Si(As)−Si(As) bond distances in $Zr(Si_{0.66}As_{0.34})Te$ increase by 0.015 Å over the corresponding distance in ZrSiTe). We believe this runs counter to the trends in atomic size of the elements, since As should be slightly smaller than Si; rather, an electronic effect is operative. Extended Hückel calculations performed on the ZrSiS-type structure showed that crystal orbitals near the Fermi level were predominantly localized on the Si square nets and that electrons added to the system enter Si−Si antibonding orbitals.[11] Unfortunately, data that would probe whether this trend holds for increased As substitution cannot be obtained due to As substitution on the Te site as well. We see no consistent explanation that accounts for the observed changes in the structural parameters of $Zr(Si_{0.5}As_{0.5})(As_{0.2}Te_{0.8})$ and $Zr(Si_{0.7}As_{0.3})(As_{0.7}Te_{0.3})$.

Materials with the ZrSiS-type structure are expected to be metallic. Four-probe single-crystal resistivity measurements show that all of the tellurides discussed in this paper do indeed show metallic behavior throughout the temperature range 77−300 K (Figure 4). Generally, the resistivities are fairly low compared with those of other metal-rich chalcogenides we have recently studied.[20,21] Assuming we can extrapolate the temperature-dependent data back to 0 K, we see that the largest residual low-temperature resistivities are exhibited by the mixed-element crystals. Of course, it is just these materials that would be expected to have the greatest defect scattering. Interestingly, the high-temperature resistivity of pure ZrSiTe is higher than those of any mixed-stoichiometry compounds and considerably higher than that of ternary ZrSnTe as well. This is despite the fact that the defect scattering seems to be quite low, judging from an extrapolation of the resistivity back to 0 K. On the contrary, it seems likely that the defect concentrations in our ZrSnTe samples are rather high for stoichiometric materials.

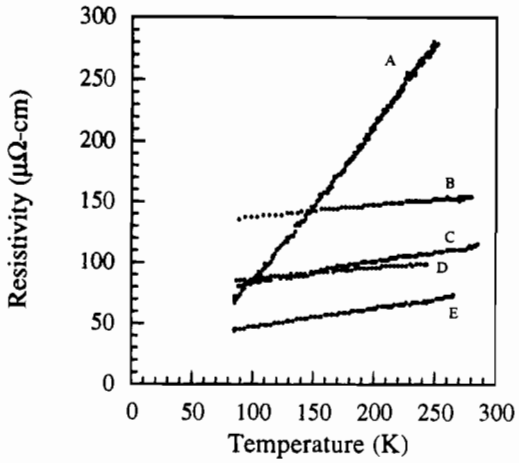

Figure 4. Single-crystal temperature-dependent resistivities of ternary and pseudoternary zirconium tellurides ZrSiTe (A), $ZrSi_{0.5}As_{0.7}Te_{0.8}$ (B), $ZrSi_{0.66}As_{0.34}Te$ (C), $ZrSi_{0.7}AsTe_{0.3}$ (D), and ZrSnTe (E).

Conclusions. The flexibility of the ZrSiS structure type has been systematically investigated for ZrZTe (Z = Si, Ge, Sn) and $ZrAs_{x+y}Si_{1-x}Te_{1-y}$ materials. In the former group, structural parameters vary smoothly in a transformation between 2-D and 3-D materials and do so in accordance with steric expectations. The Sn member of the series is new and is very much a three-dimensionally bonded compound. The As-substituted materials exhibit limited range in which As substitutes for Si only (up to approximately one-third replacement) and beyond that point As substitutes for both Si and Te. Substitution on Si sites alone leads to retention of the 2-D ZrSiTe structure; any appreciable substitution for Te seems to be accompanied by a collapse of the layered structure to a 3-D structure and formation of interlayer Zr−Te(As) bonds.

Acknowledgment. This research was generously supported by the National Science Foundation through Grant DMR-9215890 and by the Robert A. Welch Foundation through Grant A-1132. We thank Kyungsoo Ahn for assistance with the resistivity measurements. The R3m/v single-crystal X-ray diffractometer and crystallographic computing system were purchased from funds provided by the National Science Foundation (Grant CHE-8513273). We also thank Dr. Renald Guillemette for his assistance with the microprobe analyses.

Supporting Information Available: Tables of crystallographic data and anisotropic displacement parameters for ZnSnTe, $ZrSi_{0.66}As_{0.34}Te$, and $ZrSi_{0.5}As_{0.7}Te_{0.8}$ and a table of cell parameters, volumes, and *c*/*a* ratios as a function of Ge content of $ZrSi_{1-x}Ge_xTe$ solid solutions (3 pages). Ordering information is given on any current masthead page.

IC950517P

(20) Ahn, K.; Hughbanks, T. *J. Solid State Chem.* **1993**, *102*, 446.
(21) Ahn, K.; Hughbanks, T.; Rathnayaka, K. D. D.; Naugle, D. G. *Chem. Mater.* **1994**, *6*, 418−423.